JACS
JOURNAL OF THE AMERICAN CHEMICAL SOCIETY

pubs.acs.org/JACS

Article

Interplay between π-Conjugation and Exchange Magnetism in One-Dimensional Porphyrinoid Polymers

Kalyan Biswas, Maxence Urbani, Ana Sánchez-Grande, Diego Soler-Polo, Koen Lauwaet, Adam Matěj, Pingo Mutombo, Libor Veis, Jiri Brabec, Katarzyna Pernal, José M. Gallego, Rodolfo Miranda, David Écija,* Pavel Jelínek,* Tomás Torres,* and José I. Urgel*

Cite This: J. Am. Chem. Soc. 2022, 144, 12725−12731

Read Online

ACCESS | Metrics & More | Article Recommendations | Supporting Information

ABSTRACT: The synthesis of novel polymeric materials with porphyrinoid compounds as key components of the repeating units attracts widespread interest from several scientific fields in view of their extraordinary variety of functional properties with potential applications in a wide range of highly significant technologies. The vast majority of such polymers present a closed-shell ground state, and, only recently, as the result of improved synthetic strategies, the engineering of open-shell porphyrinoid polymers with spin delocalization along the conjugation length has been achieved. Here, we present a combined strategy toward the fabrication of one-dimensional porphyrinoid-based polymers homocoupled via surface-catalyzed [3 + 3] cycloaromatization of isopropyl substituents on Au(111). Scanning tunneling microscopy and noncontact atomic force microscopy describe the thermal-activated intra- and intermolecular oxidative ring closure reactions as well as the controlled tip-induced hydrogen dissociation from the porphyrinoid units. In addition, scanning tunneling spectroscopy measurements, complemented by computational investigations, reveal the open-shell character, that is, the antiferromagnetic singlet ground state ($S = 0$) of the formed polymers, characterized by singlet−triplet inelastic excitations observed between spins of adjacent porphyrinoid units. Our approach sheds light on the crucial relevance of the π-conjugation in the correlations between spins, while expanding the on-surface synthesis toolbox and opening avenues toward the synthesis of innovative functional nanomaterials with prospects in carbon-based spintronics.

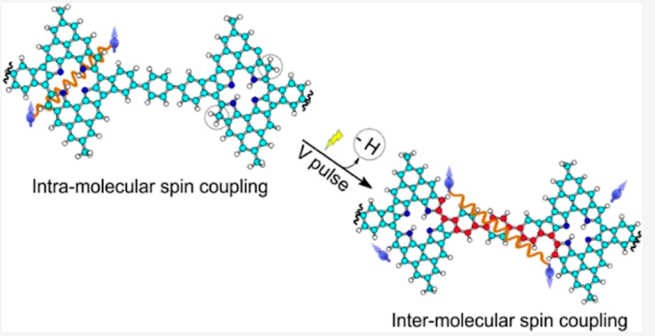

INTRODUCTION

Macrocyclic compounds based on porphyrins, that is, porphyrinoid compounds, are often under the spotlight by virtue of their inspiring biological, photophysical, and photochemical properties, being frequently recognized due to their role in energy metabolism and light harvesting in photosynthesis.[1,2] Over the last few years, their potential in a great number of technological and medical applications[3] such as photocatalysis,[4] nonlinear optics,[5] molecular photovoltaics,[6,7] spintronics,[8] drug delivery,[9,10] and biological imaging and sensing[11,12] have undoubtedly expanded their use. Interestingly enough, the properties of porphyrinoid compounds can be modulated by structural modifications in the different positions of the peripheral substituents, as well as in the heterocyclic macrocycle, where the metal center directly affects their electronic and magnetic properties.[13,14]

In the context of surface science, investigations on intramolecular conformations, intermolecular coupling and supramolecular interactions of porphyrinoids have been performed in the last few years considering the interest of scientists from different fields in the study of such compounds adsorbed on well-defined interfaces.[15−17] While great efforts have been devoted to the systematic study of intramolecular conformations and noncovalent interactions containing different metals in the macrocycle and several peripheral-functionalized substituents; the intermolecular carbon−carbon (C−C) coupling of such compounds has been mainly limited to the fabrication of on-surface polymers and oligomers via the well-known Ullmann-like coupling[18−20] or dehydrogenative coupling,[21−24] among others.[25−30] However, further on-surface investigations of alternative chemical reactions with relevant implications in organic synthesis have remained unexplored. Among the novel on-surface reactions reported recently, the surface-catalyzed [3 + 3] cycloaromatization of isopropyl and isopropenyl substituents on arenes is of particular interest providing a novel pathway toward the fabrication of polymers

Received: March 11, 2022
Published: July 11, 2022

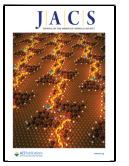

Scheme 1. On-Surface Reaction Scheme toward the Synthesis of 1D Porphyrinoid Polymers

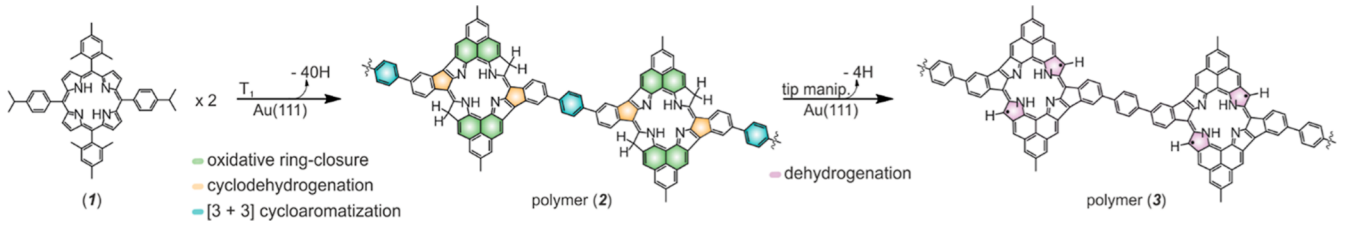

that cannot be synthetized via conventional solution chemistry.[31]

Contemporarily, the field of carbon magnetism, with important advantages over classical semiconductors and metals, has gained increased attention in view of the recent progress made following a bottom-up synthesis approach.[32] Carbon-based nanomaterials may present exceptional electronic and magnetic features conceivable to be exploited in the fabrication of multifunctional spintronic devices. Magnetism in these compounds can arise from different aspects such as: (i) edge effects, where zigzag edge topologies allow the formation of low-energy localized edge states, (ii) non-Kekulé structures formed via Coulomb repulsion between valence electrons, or (iii) spin disparity caused due to a sublattice imbalance in the bipartite lattice. The research on the fundamental properties and applications of such magnetism makes the synthesis of magnetic carbon nanomaterials an appealing research area.[33−38]

Under this scenario, the comprehensive fabrication of magnetic (open-shell) porphyrinoid-based polymers emerges as a highly appealing field of research. However, the vast majority of the porphyrinoid compounds studied to date exhibit a nonmagnetic (closed-shell) character. Radicals stabilized by spin delocalization over the π-electron systems of porphyrinoids have been rarely found both in solution and on-surface chemistry.[39] Only recently, the on-surface formation of magnetic one-dimensional (1D) oligomers and polymers based on covalently linked porphyrinoid building blocks has been achieved.[19,24] Therefore, the fabrication of innovative magnetic porphyrinoid-based polymers would constitute the basis for further development toward molecular electronics expanding the current on-surface chemistry toolbox. In this article, we introduce an exemplary approach toward the bottom-up fabrication and characterization of unprecedented magnetic porphyrinoid-based polymers homocoupled via surface-catalyzed [3 + 3] cycloaromatization of isopropyl substituents studied on Au(111) under ultrahigh vacuum (UHV) conditions. To this end, we have synthesized a porphyrin precursor (**1**) in solution that can be sublimed intact on the gold surface. Porphyrin **1** was prepared according to previously reported methods developed by Lindsey for the synthesis of *trans*-A2B2 type porphyrins[40] involving BF_3−ethanol cocatalysis.[41] The [2 + 2] condensation of 5-mesityldipyromethane[42−45] (1 equiv) and culminaldehyde (1 equiv) in $CHCl_3$ containing 0.75% ethanol in the presence of $BF_3{\cdot}Et_2O$ at room temperature (RT) for 2 h, followed by irreversible oxidation of the porphyrinogene intermediate with DDQ for an additional 1 h, afforded porphyrin **1** in 20% yield (DDQ = 2,3-dichloro-5,6-dicyano-1,4-benzoquinone). Further synthesis and characterization details are provided in the Supporting Information. Our molecular-level investigations, accomplished by means of scanning probe techniques and complemented by multidisciplinary theoretical calculations, are shown in Scheme 1. A thermal activation step ensures the intramolecular cyclodehydrogenation and oxidative ring closure reactions, as well as the intermolecular oxidative coupling, that is, [3 + 3] cycloaromatization, of **1** through isopropyl substituents, which leads to the formation of polymer **2**. Subsequent scanning tunneling microscopy (STM) tip-induced atom manipulation experiments allow the controllable cleavage of hydrogens from the two saturated carbon atoms of **2**, giving rise to polymer **3**. Interestingly, polymer **3** exhibits magnetic interactions between unpaired spins of adjacent porphyrinoid units, experimentally manifested as spin−flip excitations, revealing the crucial interplay between magnetic exchange and π-conjugation.

RESULTS AND DISCUSSION

To achieve the formation of the desired porphyrinoid polymer, precursor **1** was sublimed onto a smooth Au(111) surface held at RT under UHV conditions. Figure 1a shows a representative STM image after the sublimation of **1** on Au(111), revealing the predominant presence of several self-assembled domains stabilized by CH···π interactions between adjacent precursors coexisting with some disordered regions (see Figure S1). Annealing of the sample at 200 °C (T_1 in Scheme 1) gives rise to the efficient formation of relatively long 1D chains, where porphyrinoid units, linked to each other, can be discerned as shown in Figure 1b. To access the chemical structure of such polymers, frequency-shift noncontact atomic force microscopy (nc-AFM) images acquired with a CO-functionalized tip were performed.[46] The resulting image (Figure 1c) suggests that the thermal energy provided by annealing the sample at 200 °C is sufficient to afford a one-step reaction process toward the formation of polymer **2**. On the one hand, nc-AFM images reveal the formation of a new phenylene ring between porphyrinoid units, which arises from the intermolecular oxidative coupling of isopropyl substituents (highlighted by the dashed blue circle in Figure 1c). The mechanism of such a chemical reaction, unexpected to occur in conventional solution chemistry, has only recently been described in on-surface synthesis by the seminal publication of Kinikar et al.[31] On the other hand, two intramolecular reactions took place: (i) oxidative ring closure of the four methyl substituents per porphyrinoid unit, providing four hexagonal rings (highlighted by the dashed green circle in Figure 1c) and (ii) cyclodehydrogenation of the phenyl groups adjacent to the isopropyl substituents, which admit two equal rotation possibilities upon activation, affording the formation of two five-membered rings (highlighted by the dashed orange circle in Figure 1c). In addition, four features of increased frequency shift per porphyrinoid unit are identified (white arrows in Figure 1c). Such features are typically attributed to hydrogens linked to unsaturated carbon atoms adopting a nonplanar configuration. Notably, the extra-hydrogenation of the two

https://doi.org/10.1021/jacs.2c02700
J. Am. Chem. Soc. 2022, 144, 12725−12731

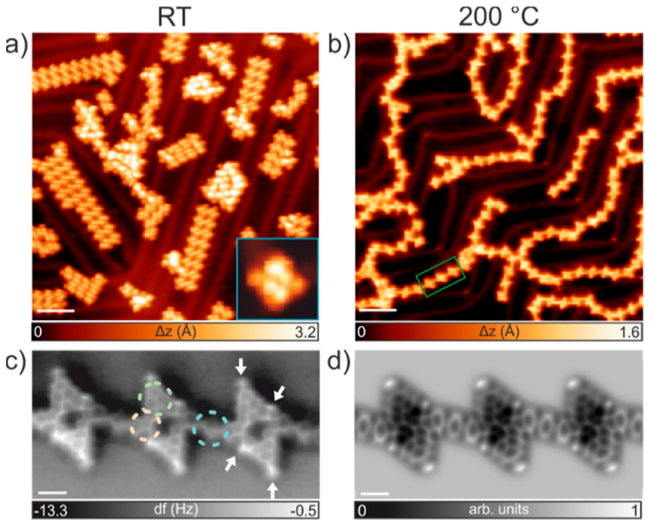

Figure 1. Synthesis and structural characterization of polymer **2** on Au(111). (a) Overview STM topography image of the Au(111) surface after RT deposition of **1**, showing the formation of self-assembled islands coexisting with some disordered regions. V_b = −1.0 V, I_t = 100 pA, scale bar = 5 nm. The inset shows a high-resolution STM image of an individual molecule where four bright protrusions of identical apparent height are attributed to the tilt of the four peripheral benzene rings due to steric hindrance with the porphyne backbone. Image size 3.5 nm × 3.5 nm, V_b = −0.5 V, I_t = 50 pA. (b) Overview STM topography image showing the formation of 1D chains (polymer **2**) after deposition of **1** and subsequent annealing at 200 °C. V_b = 0.5 V, I_t = 110 pA, scale bar = 5 nm. (c) Constant-height frequency-shift nc-AFM image acquired with a CO-functionalized tip (z offset −43 pm below STM set point = 5 mV, 50 pA), scale bar = 1 nm. The dashed circles and white arrows highlight the chemical reactions resulted from the annealing of **1** at 200 °C and the out-of-plane hydrogens attached to unsaturated carbon atoms, respectively (see Scheme 1). (d) Simulated nc-AFM image of (c). Scale bar = 1 nm.

carbon atoms at the apex of the five-membered rings was unexpected and is attributed to the presence of hydrogen on the surface, being available to passivate the most reactive sites of the studied compounds. Such experimental features are well reproduced by the corresponding nc-AFM simulations[47] of polymer **2** (Figure 1d), which further support the highly nonplanar configuration of several hydrogens with respect to the underlying surface.

Further annealing of the sample at 280 °C affords the partial cleavage of the aforementioned hydrogen atoms, though the applied thermal energy is also compatible with the unselective C−H bond dissociation of other segments of polymer **2** (see Figure S2). Thus, to achieve the fabrication of polymer **3**, STM tip-induced atom manipulation experiments were performed, in agreement with previous works.[33,48−53] Figure 2a,b shows a profound difference between constant-height STM images of a polymer segment before and after the tip-induced manipulation event, which anticipates a modification of its electronic properties. The successful removal of one of the two hydrogens in each sp^3 carbon site is further confirmed by the corresponding nc-AFM images (Figure 2c,d), where the absence of the bright features located at the apex of the six five-membered rings after the tip manipulation is clearly discerned (highlighted with white arrows). Therefore, as anticipated in Scheme 1, every hydrogen dissociation step introduces one delocalized π radical into the system.

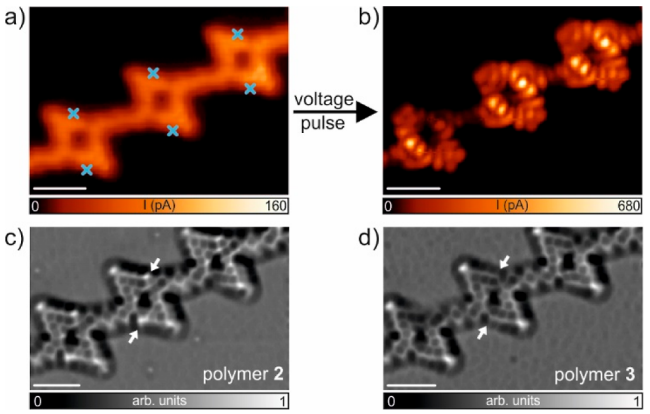

Figure 2. Transformation of polymer **2** into polymer **3** via STM tip-induced hydrogen dissociation. (a,b) High-resolution constant-height STM images acquired with a CO-functionalized tip that show the generation of polymer **3** through voltage-pulse-induced dissociation of individual hydrogen atoms from polymer **2**. The blue crosses specified the positions of the tip where the voltage pulse was performed. V_b = 5 mV, I_t = 30 pA. (c,d) Laplace-filtered constant-height frequency-shift nc-AFM images of (a,b) that evidences the absence of the bright protrusion (two per porphyrinoid unit) after the tip manipulation event, which is assigned to the controlled dissociation of one hydrogen atom per carbon site. The white arrows highlight the presence (c) and absence (d) of such bright protrusion. z offset −50 pm below STM set point = 5 mV, 40 pA. All scale bars = 1 nm.

Furthermore, the planar appearance shown in the scanning probe experiments together with density functional theory (DFT)[54] calculations evidence that polymer **3** is physisorbed on the gold surface (see Figure S3).

In addition to the detailed structural investigation of polymers **2** and **3**, we have performed scanning tunneling spectroscopy (STS) measurements to probe the electronic structure of the resulting polymers on Au(111). Long-range differential conductance dI/dV spectra acquired on polymers **2** and **3** display strong features in the density of states at −0.63 and +0.85, and −0.85 and +0.90 V respectively, which are assigned to the valence band (VB) maximum and the conduction band (CB) minimum, corresponding to STS band gaps of 1.48 and 1.75 eV (see Figure S4). The experimental dI/dV maps acquired at the energy positions specified in Figure S4a,c allow resolving the spatial distribution of the VB and the CB, which match well with the simulated dI/dV maps of the frontier bands[55] calculated for a free-standing infinite segment of polymers **2** and **3** using DFT (Figure S4b,d).

Next, in order to obtain information about the transition from nonmagnetic to magnetic nature of polymers **2** and **3**, respectively, we have performed a detailed analysis of the low-bias dI/dV spectra (in a range of ±50 mV), where the appearance of low-energy spectral features can be associated with a magnetic fingerprint.[33−38] First, we have inspected a segment of polymer **2**. Herein, no spectral features were observed, as shown in Figure 3a. However, this scenario is drastically modified after tip-induced dehydrogenation at the positions specified in the STM images shown in Figure 3a−c.

After a first tip-induced hydrogen dissociation event at positions α and β shown in the chemical sketch in Figure 3a (realized with the tip located at the center of the porphyrinoid unit), two zero-energy excitation features mainly located at the five-membered rings appear. Such features are typically

https://doi.org/10.1021/jacs.2c02700
J. Am. Chem. Soc. 2022, 144, 12725−12731

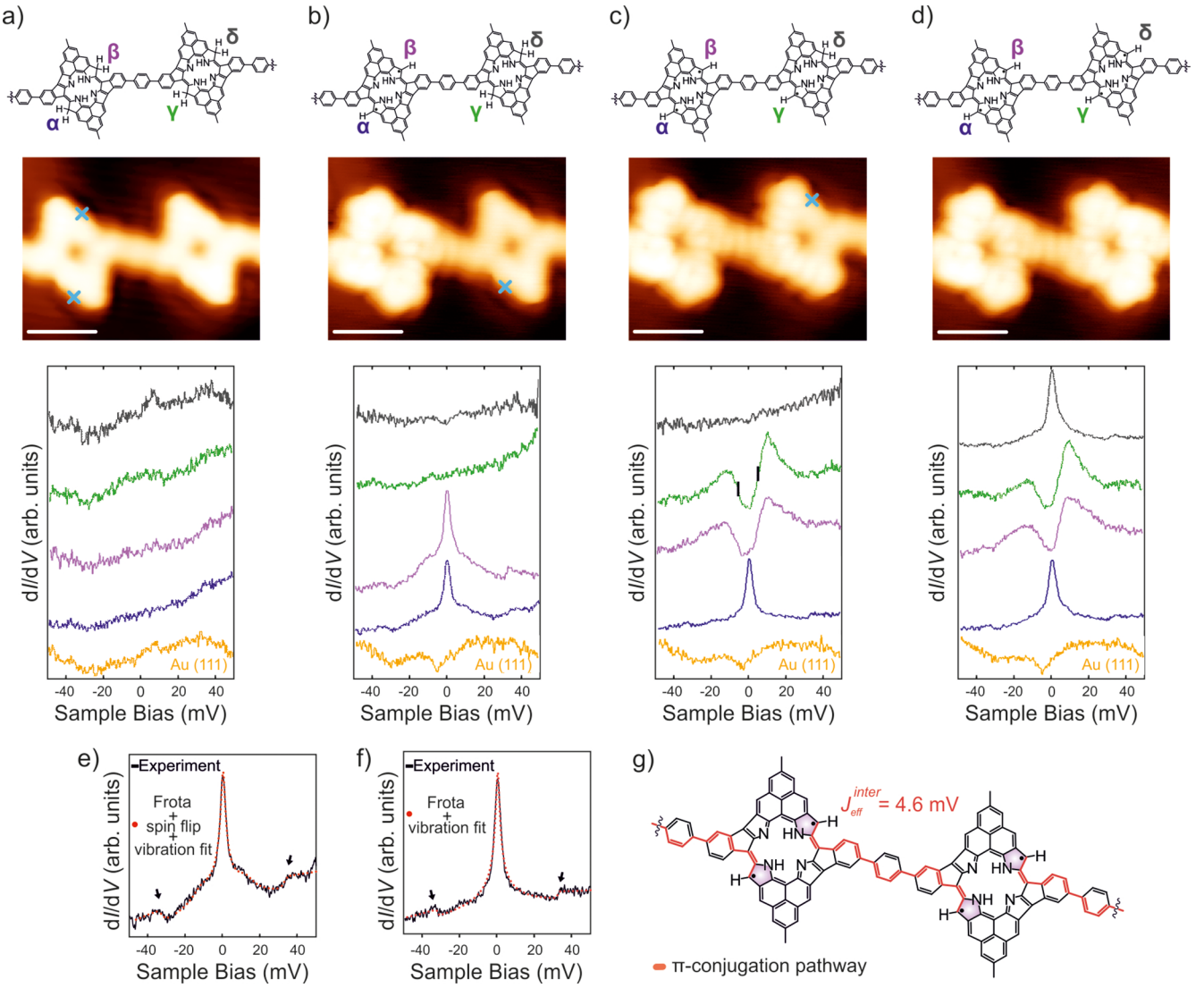

Figure 3. Intra- and intermolecular characterization of the magnetic coupling of 1D porphyrinoid polymers on Au(111). (a–d) Chemical sketches, constant-current STM images, and low-bias dI/dV spectra acquired at positions α–δ (depicted in the chemical sketches) upon the sequential dissociation of hydrogens from the unsaturated carbon atoms at the five-membered rings of each porphyrinoid unit. The blue crosses shown in the STM images indicate the position, where the tip-induced manipulation was performed. The orange curve corresponds to the reference dI/dV spectrum acquired on Au(111). The two black rectangles in the green spectrum displayed in (c) highlight the inelastic excitation threshold obtained at the half maximum width, i.e., ±4.6 mV, of the observed resonances. STM images: V_b = 5 mV, I_t = 30 pA, scale bars = 1 nm. dI/dV spectra: (V_b = 50 mV, I_t = 0.45 nA, and V_{rms} = 0.8 mV) (e) dI/dV spectrum shown in position α of (b), fitted using the Frota function including the vibration plus spin-flip fits (red line). Clearly, the fit reproduces the observed spectral features, which further support the existence of a ferromagnetic (triplet) ground state of a porphyrinoid unit predicted by DFT calculations. (f) dI/dV spectrum shown in position α of (c) showing the nice fitting (red dashed line) to a single Frota function. The fit is now very satisfactory without the spin–flip component. The black arrows shown in (e,f) highlight the vibrations associated with the CO molecule used to functionalize the tip observed at ~±32 mV (g) Chemical sketch of polymer **3**. The red line highlights the π-conjugation pathway between porphyrinoid units.

characteristic of a Kondo resonance (total spin S = 1/2)[56] or attributed to ferromagnetic correlations (triplet ground state, S = 1).[37,57−59] To unravel their nature, we have performed DFT as well as many-body calculations of a porphyrine unit revealing the triplet ground state of the porphyrinoid unit once the two extra hydrogens located at positions α and β are removed (see Figures S5−S8, Table S1 and underlying discussion in the Supporting Information for further details). Furthermore, the fit of the experimental data corroborates the theoretical predictions about the triplet ground state in the porphyrinoid unit, resulting in a ferromagnetic intraporphyrin coupling (Figures 3e and S9a, where the fittings of the spectra from Figure 3b acquired on top of α and β are shown). Notably, a single Frota line shape, that is well-known to fit Kondo resonances, cannot fit our experimental spectra over the whole voltage range shown. Instead, an underscreened S = 1 Kondo with spin-flip signatures does lead to a good fit (exchange coupling energy of J_{eff} = 11.9 meV derived from the fit, Table S2), in agreement with the theoretically predicted S = 1 ground state. In addition, we have investigated the anisotropy of the current-induced density (ACID),[60] which has proven to be an extremely versatile and descriptive method used to analyze the density of delocalized electrons in ground state molecules and polymers.[61] ACID calculations performed on a single basic unit of polymer **3** suggest that the two formed five-membered rings (colored in orange in Scheme 1) show a clear

https://doi.org/10.1021/jacs.2c02700
J. Am. Chem. Soc. 2022, 144, 12725−12731

paratropic contribution in the delocalized π-system, while the remaining parts reveal a diatropic current around their peripheries. The picture depicted by the ACID calculations in Figure S7a can be intuitively explained by the fact that the phenalene subunits formed upon the intramolecular ring closure impose the break of the π-conjugation pathway, largely influencing the chemical reactivity as well as the electronic and magnetic properties of the polymer (see the Supporting Information for detailed discussion).

Further hydrogen dissociation realized on an adjacent porphyrinoid unit (position γ in Figure 3a−d) unveils a new scenario. Low-bias dI/dV spectra acquired at positions β and γ reveal a conductance step at ±4.6 mV, symmetric with respect to the Fermi energy, indicative of inelastic excitations (Figure 3c,d). Such inelastic excitations are ascribed to spin excitations (singlet−triplet magnetic excitation due to the tunneling electrons), where the two closer spins from adjacent porphyrinoid units are antiferromagnetically coupled, with an effective exchange parameter J_{eff} = 4.6 mV, in good agreement with the calculated J_{eff} = 7 mV (see Figure S10 and Table S3 for a dimer model adopted to estimate the effective magnetic exchange interactions between the individual radical states). Remarkably, the low-bias dI/dV spectrum repeated at position α in Figure 3c presents a single peak at the Fermi energy that, in contrast to the previous spectrum acquired on α prior to the removal of the extra hydrogen at position γ (Figure 3b), now it is well fitted to a single Frota peak centered at the Fermi level (Figure 3f). We assign this feature to a Kondo resonance (S = 1/2) of an unpaired electron spin located at position α. The disappearance here of the spin−flip signal (Figure S9c) is attributed to the prevalence of the antiferromagnetic coupling between adjacent porphyrinoid units (between positions β and γ from Figure 3), over the previous ferromagnetic coupling between α and β. Such prevalence is tentatively related to the formation of a π-conjugated path between β and γ.

Finally, we have performed tip-induced hydrogen dissociation experiments in order to cleavage one of the two hydrogens located at position δ (Figure 3a−d). Herein, as expected, the low-bias dI/dV spectrum obtained at position δ reveals a zero-energy excitation with an identical shape to the one observed for position α in Figure 3c,d, while maintaining the antiferromagnetic coupling between β and γ. Therefore, we can conclude that the oxidative coupling of isopropyl substituents, that is, formation of a benzene ring and subsequent tip-induced dehydrogenation, provides a π-conjugated pathway between unpair spins of adjacent porphyrinoid units, which allows their antiferromagnetic coupling (see the sketch in Figure 3g).

CONCLUSIONS

We have demonstrated an illustrative approach toward the fabrication of magnetic porphyrinoid-based 1D polymers on the Au(111) surface. Polymer **2** is achieved by thermal activation of precursor **1** at 200 °C, which induces the expected intramolecular oxidative ring closure and cyclodehydrogenation reactions; while an intermolecular oxidative coupling, that is, [3 + 3] cycloaromatization via isopropyl substituents provides the linkage between porphyrinoid units. Successive STM single-atom manipulation experiments ensure the controllable dissociation of hydrogen atoms from the saturated carbon atoms of polymer **2**, promoting the formation of polymer **3**. The chemical structures of both polymers have been clearly elucidated by STM and nc-AFM. In addition, a detailed electronic characterization, performed by STS measurements and DFT calculations, reveals a nonmagnetic ground state for polymer **2** as no spectral features in the low-bias regime were detected. Interestingly, the removal of hydrogens from the two unsaturated carbon atoms at the five-membered rings of a porphyrinoid unit reveals zero-energy excitation features ascribed to its triplet ground state (S = 1). However, further tip-induced hydrogen dissociation experiments performed at adjacent units unveils a scenario, where an antiferromagnetic coupling, distinguished by an experimental exchange-coupling strength of 4.6 meV, is observed between the two closer spins from adjacent porphyrinoid units. Our work highlights the relevance of the π-conjugation in the correlations between spins, representing a profitable step toward the on-surface synthesis of covalently linked 1D magnetic polymers with application prospects in nanoscale spintronic devices. In more general terms, we envision that our on-surface synthetic approach can be expanded to the controlled fabrication of two-dimensional magnetic polymers by further rationalization of the precursor chemical design.

ASSOCIATED CONTENT

Supporting Information

The Supporting Information is available free of charge at https://pubs.acs.org/doi/10.1021/jacs.2c02700.

Experimental details; synthesis; characterizations; computational studies; and NMR spectra (PDF)

AUTHOR INFORMATION

Corresponding Authors

David Écija − *IMDEA Nanoscience, Madrid 28049, Spain;* orcid.org/0000-0002-8661-8295; Email: david.ecija@imdea.org

Pavel Jelínek − *Institute of Physics of the Czech Academy of Science, Praha 162 00, Czech Republic; Regional Centre of Advanced Technologies and Materials, Czech Advanced Technology and Research Institute (CATRIN), Palacký University Olomouc, Olomouc 783 71, Czech Republic;* orcid.org/0000-0002-5645-8542; Email: jelinekp@fzu.cz

Tomás Torres − *IMDEA Nanoscience, Madrid 28049, Spain; Departamento de Química Orgánica and Institute for Advanced Research in Chemistry (IAdChem), Universidad Autónoma de Madrid, Madrid 28049, Spain;* orcid.org/0000-0001-9335-6935; Email: tomas.torres@uam.es

José I. Urgel − *IMDEA Nanoscience, Madrid 28049, Spain;* orcid.org/0000-0001-7608-2979; Email: jose-ignacio.urgel@imdea.org

Authors

Kalyan Biswas − *IMDEA Nanoscience, Madrid 28049, Spain*

Maxence Urbani − *IMDEA Nanoscience, Madrid 28049, Spain;* orcid.org/0000-0001-7733-6440

Ana Sánchez-Grande − *IMDEA Nanoscience, Madrid 28049, Spain*

Diego Soler-Polo − *Institute of Physics of the Czech Academy of Science, Praha 162 00, Czech Republic;* orcid.org/0000-0001-9215-4151

Koen Lauwaet − *IMDEA Nanoscience, Madrid 28049, Spain*

Adam Matěj − *Institute of Physics of the Czech Academy of Science, Praha 162 00, Czech Republic; Regional Centre of Advanced Technologies and Materials, Czech Advanced*

Technology and Research Institute (CATRIN), Palacký University Olomouc, Olomouc 783 71, Czech Republic

Pingo Mutombo − *Institute of Physics of the Czech Academy of Science, Praha 162 00, Czech Republic*

Libor Veis − *J. Heyrovský Institute of Physical Chemistry, Czech Academy of Sciences, Prague 182 00, Czech Republic;* orcid.org/0000-0002-4229-6335

Jiri Brabec − *J. Heyrovský Institute of Physical Chemistry, Czech Academy of Sciences, Prague 182 00, Czech Republic;* orcid.org/0000-0002-7764-9890

Katarzyna Pernal − *Institute of Physics, Lodz University of Technology, Lodz 90-924, Poland;* orcid.org/0000-0003-1261-9065

José M. Gallego − *Instituto de Ciencia de Materiales de Madrid, CSIC, Madrid 28049, Spain;* orcid.org/0000-0003-1716-0126

Rodolfo Miranda − *IMDEA Nanoscience, Madrid 28049, Spain; Departamento de Física de La Materia Condensada, Universidad Autónoma de Madrid, Madrid 28049, Spain*

Complete contact information is available at: https://pubs.acs.org/10.1021/jacs.2c02700

Notes

The authors declare no competing financial interest.

■ ACKNOWLEDGMENTS

IMDEA Nanociencia acknowledges support from the "Severo Ochoa" Program for Centers of Excellence in R&D (MINECO, grant SEV-2016-0686). We appreciate support from the Praemium Academie of the Academy of Science of the Czech Republic and the CzechNanoLab Research Infrastructure supported by MEYS CR (LM2018110). D.E. thanks funding from ERC Consolidator Grant ELECNANO (no. 766555) and Ministerio de Ciencia e Innovación (PID2019-108532GB-I00). K.P. acknowledges the support of the National Science Center of Poland under grant no. 2019/35/B/ST4/01310. P.J. thanks the support of the GACR 20-13692X. J.B. acknowledges the support of the GACR 19-13126Y. J.I.U. thanks the funding from the European Union's Horizon 2020 research and innovation program under the Marie Skłodowska-Curie grant agreement no. [886314].

■ REFERENCES

(1) Kadish, K.; Smith, K. M.; Guilard, R. *The Porphyrin Handbook*; Elsevier, 2000; Vol. *10*, pp 1−254.

(2) Kadish, K. M.; Guilard, R.; Smith, K. M. *Handbook of Porphyrin Science: With Applications to Chemistry, Physics, Materials Science, Engineering, Biology and Medicine*; World Scientific, 2012; Vol. *18*, pp 1−472.

(3) Zhang, Y.; Lovell, J. F. Porphyrins as Theranostic Agents from Prehistoric to Modern Times. *Theranostics* **2012**, *2*, 905−915.

(4) Chen, Y.; Li, A.; Huang, Z.-H.; Wang, L.-N.; Kang, F. Porphyrin-Based Nanostructures for Photocatalytic Applications. *Nanomaterials* **2016**, *6*, 51.

(5) Senge, M. O.; Fazekas, M.; Notaras, E. G. A.; Blau, W. J.; Zawadzka, M.; Locos, O. B.; Ni Mhuircheartaigh, E. M. Nonlinear Optical Properties of Porphyrins. *Adv. Mater.* **2007**, *19*, 2737−2774.

(6) Li, L.-L.; Diau, E. W.-G. Porphyrin -Sensitized Solar Cells. *Chem. Soc. Rev.* **2013**, *42*, 291−304.

(7) Urbani, M.; Grätzel, M.; Nazeeruddin, M. K.; Torres, T. Meso-Substituted Porphyrins for Dye-Sensitized Solar Cells. *Chem. Rev.* **2014**, *114* (24), 12330−12396.

(8) Lopes, D. M.; Araujo-Chaves, J. C.; Menezes, L. R.; Nantes-Cardoso, I. L. *Technological Applications of Porphyrins and Related Compounds: Spintronics and Micro-/Nanomotors*; IntechOpen, 2019; pp 1−236.

(9) Huang, H.; Song, W.; Rieffel, J.; Lovell, J. F. Emerging Applications of Porphyrins in Photomedicine. *Front. Physiol.* **2015**, *3*, 23.

(10) Bechet, D.; Couleaud, P.; Frochot, C.; Viriot, M.-L.; Guillemin, F.; Barberi-Heyob, M. Nanoparticles as Vehicles for Delivery of Photodynamic Therapy Agents. *Trends Biotechnol.* **2008**, *26*, 612−621.

(11) Ding, Y.; Zhu, W.-H.; Xie, Y. Development of Ion Chemosensors Based on Porphyrin Analogues. *Chem. Rev.* **2017**, *117*, 2203−2256.

(12) Josefsen, L. B.; Boyle, R. W. Unique Diagnostic and Therapeutic Roles of Porphyrins and Phthalocyanines in Photodynamic Therapy, Imaging and Theranostics. *Theranostics* **2012**, *2*, 916−966.

(13) Hiroto, S.; Miyake, Y.; Shinokubo, H. Synthesis and Functionalization of Porphyrins through Organometallic Methodologies. *Chem. Rev.* **2017**, *117*, 2910−3043.

(14) Senge, M. O. Stirring the Porphyrin Alphabet Soup—Functionalization Reactions for Porphyrins. *Chem. Commun.* **2011**, *47*, 1943−1960.

(15) Auwärter, W.; Écija, D.; Klappenberger, F.; Barth, J. V. Porphyrins at Interfaces. *Nat. Chem.* **2015**, *7*, 105−120.

(16) Gottfried, J. M. Surface Chemistry of Porphyrins and Phthalocyanines. *Surf. Sci. Rep.* **2015**, *70*, 259−379.

(17) Otsuki, J. STM Studies on Porphyrins. *Coord. Chem. Rev.* **2010**, *254*, 2311−2341.

(18) Mateo, L. M.; Sun, Q.; Eimre, K.; Pignedoli, C. A.; Torres, T.; Fasel, R.; Bottari, G. On-Surface Synthesis of Singly and Doubly Porphyrin-Capped Graphene Nanoribbon Segments. *Chem. Sci.* **2021**, *12*, 247−252.

(19) Mallada, B.; Błoński, P.; Langer, R.; Jelínek, P.; Otyepka, M.; de la Torre, B. On-Surface Synthesis of One-Dimensional Coordination Polymers with Tailored Magnetic Anisotropy. *ACS Appl. Mater. Interfaces* **2021**, *13*, 32393−32401.

(20) Lafferentz, L.; Eberhardt, V.; Dri, C.; Africh, C.; Comelli, G.; Esch, F.; Hecht, S.; Grill, L. Controlling On-Surface Polymerization by Hierarchical and Substrate-Directed Growth. *Nat. Chem.* **2012**, *4*, 215−220.

(21) Wiengarten, A.; Seufert, K.; Auwärter, W.; Ecija, D.; Diller, K.; Allegretti, F.; Bischoff, F.; Fischer, S.; Duncan, D. A.; Papageorgiou, A. C.; Klappenberger, F.; Acres, R. G.; Ngo, T. H.; Barth, J. V. Surface-Assisted Dehydrogenative Homocoupling of Porphine Molecules. *J. Am. Chem. Soc.* **2014**, *136*, 9346−9354.

(22) He, Y.; Garnica, M.; Bischoff, F.; Ducke, J.; Bocquet, M.-L.; Batzill, M.; Auwärter, W.; Barth, J. V. Fusing Tetrapyrroles to Graphene Edges by Surface-Assisted Covalent Coupling. *Nat. Chem.* **2017**, *9*, 33−38.

(23) Krasnikov, S. A.; Doyle, C. M.; Sergeeva, N. N.; Preobrajenski, A. B.; Vinogradov, N. A.; Sergeeva, Y. N.; Zakharov, A. A.; Senge, M. O.; Cafolla, A. A. Formation of Extended Covalently Bonded Ni Porphyrin Networks on the Au(111) Surface. *Nano Res.* **2011**, *4*, 376−384.

(24) Sun, Q.; Mateo, L. M.; Robles, R.; Lorente, N.; Ruffieux, P.; Bottari, G.; Torres, T.; Fasel, R. Bottom-up Fabrication and Atomic-Scale Characterization of Triply Linked, Laterally π-Extended Porphyrin Nanotapes. *Angew. Chem., Int. Ed.* **2021**, *60*, 16208−16214.

(25) Saywell, A.; Browning, A. S.; Rahe, P.; Anderson, H. L.; Beton, P. H.; Beton, H. Organisation and Ordering of 1D Porphyrin Polymers Synthesised by On-Surface Glaser Coupling. *Chem. Commun.* **2016**, *52*, 10342−10345.

(26) Tanoue, R.; Higuchi, R.; Ikebe, K.; Uemura, S.; Kimizuka, N.; Stieg, A. Z.; Gimzewski, J. K.; Kunitake, M. Thermodynamic Self-Assembly of Two-Dimensional π -Conjugated Metal−Porphyrin Covalent Organic Frameworks by "On-Site" Equilibrium Polymerization. *J. Nanosci. Nanotechnol.* **2014**, *14*, 2211−2216.

(27) Liu, X.-H.; Guan, C.-Z.; Zheng, Q.-N.; Wang, D.; Wan, L.-J. Molecular Engineering of Schiff-Base Linked Covalent Polymers with

Diverse Topologies by Gas-Solid Interface Reaction. *J. Chem. Phys.* **2015**, *142*, 101905.
(28) Sahabudeen, H.; Qi, H.; Ballabio, M.; Položij, M.; Olthof, S.; Shivhare, R.; Jing, Y.; Park, S.; Liu, K.; Zhang, T.; Ma, J.; Rellinghaus, B.; Mannsfeld, S.; Heine, T.; Bonn, M.; Cánovas, E.; Zheng, Z.; Kaiser, U.; Dong, R.; Feng, X. Highly Crystalline and Semiconducting Imine-Based Two-Dimensional Polymers Enabled by Interfacial Synthesis. *Angew. Chem., Int. Ed.* **2020**, *132*, 6084−6092.
(29) Joshi, T.; Chen, C.; Li, H.; Diercks, C. S.; Wang, G.; Waller, P. J.; Li, H.; Bredas, J. L.; Yaghi, O. M.; Crommie, M. F. Local Electronic Structure of Molecular Heterojunctions in a Single-Layer 2D Covalent Organic Framework. *Adv. Mater.* **2019**, *31*, 1805941.
(30) Bischoff, F.; He, Y.; Riss, A.; Seufert, K.; Auwärter, W.; Barth, J. V. Exploration of Interfacial Porphine Coupling Schemes and Hybrid Systems by Bond-Resolved Scanning Probe Microscopy. *Angew. Chem., Int. Ed.* **2018**, *130*, 16262−16267.
(31) Kinikar, A.; Di Giovannantonio, M.; Urgel, J. I.; Eimre, K.; Qiu, Z.; Gu, Y.; Jin, E.; Narita, A.; Wang, X.-Y.; Müllen, K.; Ruffieux, P.; Pignedoli, C. A.; Fasel, R. On-Surface Polyarylene Synthesis by Cycloaromatization of Isopropyl Substituents. *Nat. Synth.* **2022**, *1*, 289−296.
(32) Yazyev, O. V. Emergence of Magnetism in Graphene Materials and Nanostructures. *Rep. Prog. Phys.* **2010**, *73*, 056501.
(33) Mishra, S.; Beyer, D.; Eimre, K.; Kezilebieke, S.; Berger, R.; Gröning, O.; Pignedoli, C. A.; Müllen, K.; Liljeroth, P.; Ruffieux, P.; Feng, X.; Fasel, R. Topological Frustration Induces Unconventional Magnetism in a Nanographene. *Nat. Nanotechnol.* **2020**, *15*, 22−28.
(34) Mishra, S.; Catarina, G.; Wu, F.; Ortiz, R.; Jacob, D.; Eimre, K.; Ma, J.; Pignedoli, C. A.; Feng, X.; Ruffieux, P.; Fernández-Rossier, J.; Fasel, R. Observation of Fractional Edge Excitations in Nanographene Spin Chains. *Nature* **2021**, *598*, 287−292.
(35) Mishra, S.; Yao, X.; Chen, Q.; Eimre, K.; Gröning, O.; Ortiz, R.; Di Giovannantonio, M.; Sancho-García, J. C.; Fernández-Rossier, J.; Pignedoli, C. A.; Müllen, K.; Ruffieux, P.; Narita, A.; Fasel, R. Large Magnetic Exchange Coupling in Rhombus-Shaped Nanographenes with Zigzag Periphery. *Nat. Chem.* **2021**, *13*, 581−586.
(36) Li, J.; Sanz, S.; Corso, M.; Choi, D. J.; Peña, D.; Frederiksen, T.; Pascual, J. I. Single Spin Localization and Manipulation in Graphene Open-Shell Nanostructures. *Nat. Commun.* **2019**, *10*, 200.
(37) Li, J.; Sanz, S.; Castro-Esteban, J.; Vilas-Varela, M.; Friedrich, N.; Frederiksen, T.; Peña, D.; Pascual, J. I. Uncovering the Triplet Ground State of Triangular Graphene Nanoflakes Engineered with Atomic Precision on a Metal Surface. *Phys. Rev. Lett.* **2020**, *124*, 177201.
(38) Sánchez-Grande, A.; Urgel, J. I.; Cahlík, A.; Santos, J.; Edalatmanesh, S.; Rodríguez-Sánchez, E.; Lauwaet, K.; Mutombo, P.; Nachtigallová, D.; Nieman, R.; Lischka, H.; de la Torre, B.; Miranda, R.; Gröning, O.; Martín, N.; Jelínek, P.; Écija, D. Diradical Organic One-Dimensional Polymers Synthesized on a Metallic Surface. *Angew. Chem.* **2020**, *59*, 17594−17599.
(39) Shimizu, D.; Osuka, A. Porphyrinoids as a Platform of Stable Radicals. *Chem. Sci.* **2018**, *9*, 1408−1423.
(40) Littler, B. J.; Ciringh, Y.; Lindsey, J. S. Investigation of Conditions Giving Minimal Scrambling in the Synthesis of Trans-Porphyrins from Dipyrromethanes and Aldehydes. *J. Org. Chem.* **1999**, *64*, 2864−2872.
(41) Lindsey, J. S.; Wagner, R. W. Investigation of the Synthesis of Ortho-Substituted Tetraphenylporphyrins. *J. Org. Chem.* **1989**, *54*, 828−836.
(42) Lee, C.-H.; Lindsey, J. S. One-Flask Synthesis of Meso-Substituted Dipyrromethanes and Their Application in the Synthesis of Trans-Substituted Porphyrin Building Blocks. *Tetrahedron* **1994**, *50*, 11427−11440.
(43) Sobral, A. J. F. N.; Rebanda, N. G. C. L.; da Silva, M.; Lampreia, S. H.; Ramos Silva, M.; Beja, A. M.; Paixão, J. A.; Rocha Gonsalves, A. M. d. A. One-Step Synthesis of Dipyrromethanes in Water. *Tetrahedron Lett.* **2003**, *44*, 3971−3973.
(44) Rohand, T.; Dolusic, E.; Ngo, T. H.; Maes, W.; Dehaen, W. Efficient Synthesis of Aryldipyrromethanes in Water and Their Application in the Synthesis of Corroles and Dipyrromethenes. *Arkivoc* **2007**, *2007*, 307−324.
(45) Zoli, L.; Cozzi, P. G. Electrophilic Activation of Aldehydes "On Water": A Facile Route to Dipyrromethanes. *ChemSusChem* **2009**, *2*, 218−220.
(46) Gross, L.; Mohn, F.; Moll, N.; Liljeroth, P.; Meyer, G. The Chemical Structure of a Molecule Resolved by Atomic Force Microscopy. *Science* **2009**, *325*, 1110−1114.
(47) Hapala, P.; Kichin, G.; Wagner, C.; Tautz, F. S.; Temirov, R.; Jelínek, P. Mechanism of High-Resolution STM/AFM Imaging with Functionalized Tips. *Phys. Rev. B: Condens. Matter Mater. Phys.* **2014**, *90*, 085421.
(48) Lohr, T. G.; Urgel, J. I.; Eimre, K.; Liu, J.; Di Giovannantonio, M.; Mishra, S.; Berger, R.; Ruffieux, P.; Pignedoli, C. A.; Fasel, R.; Feng, X. On-Surface Synthesis of Non-Benzenoid Nanographenes by Oxidative Ring-Closure and Ring-Rearrangement Reactions. *J. Am. Chem. Soc.* **2020**, *142*, 13565−13572.
(49) Sun, Q.; Mateo, L. M.; Robles, R.; Ruffieux, P.; Lorente, N.; Bottari, G.; Torres, T.; Fasel, R. Inducing Open-Shell Character in Porphyrins through Surface-Assisted Phenalenyl π-Extension. *J. Am. Chem. Soc.* **2020**, *142*, 18109−18117.
(50) Di Giovannantonio, M.; Eimre, K.; Yakutovich, A. V.; Chen, Q.; Mishra, S.; Urgel, J. I.; Pignedoli, C. A.; Ruffieux, P.; Müllen, K.; Narita, A.; Fasel, R. On-Surface Synthesis of Antiaromatic and Open-Shell Indeno[2,1-b]Fluorene Polymers and Their Lateral Fusion into Porous Ribbons. *J. Am. Chem. Soc.* **2019**, *141*, 12346−12354.
(51) Di Giovannantonio, M.; Chen, Q.; Urgel, J. I.; Ruffieux, P.; Pignedoli, C. A.; Müllen, K.; Narita, A.; Fasel, R. On-Surface Synthesis of Oligo(Indenoindene). *J. Am. Chem. Soc.* **2020**, *142*, 12925−12929.
(52) Sánchez-Grande, A.; Urgel, J. I.; Veis, L.; Edalatmanesh, S.; Santos, J.; Lauwaet, K.; Mutombo, P.; Gallego, J. M.; Brabec, J.; Beran, P.; Nachtigallová, D.; Miranda, R.; Martín, N.; Jelínek, P.; Écija, D. Unravelling the Open-Shell Character of Peripentacene on Au(111). *J. Phys. Chem. Lett.* **2021**, *12*, 330−336.
(53) Zhao, Y.; Jiang, K.; Li, C.; Liu, Y.; Xu, C.; Zheng, W.; Guan, D.; Li, Y.; Zheng, H.; Liu, C.; Luo, W.; Jia, J.; Zhuang, X.; Wang, S. Precise Control of π-Electron Magnetism in Metal-Free Porphyrins. *J. Am. Chem. Soc.* **2020**, *142*, 18532−18540.
(54) Blum, V.; Gehrke, R.; Hanke, F.; Havu, P.; Havu, V.; Ren, X.; Reuter, K.; Scheffler, M. Ab Initio Molecular Simulations with Numeric Atom-Centered Orbitals. *Comput. Phys. Commun.* **2009**, *180*, 2175−2196.
(55) Krejčí, O.; Hapala, P.; Ondráček, M.; Jelínek, P. Principles and Simulations of High-Resolution STM Imaging with a Flexible Tip Apex. *Phys. Rev. B* **2017**, *95*, 045407.
(56) Madhavan, V.; Chen, W.; Jamneala, T.; Crommie, M. F.; Wingreen, N. S. Tunneling into a Single Magnetic Atom: Spectroscopic Evidence of the Kondo Resonance. *Science* **1998**, *280*, 567−569.
(57) Sasaki, S.; De Franceschi, S.; Elzerman, J. M.; van der Wiel, W. G.; Eto, M.; Tarucha, S.; Kouwenhoven, L. P. Kondo Effect in an Integer-Spin Quantum Dot. *Nature* **2000**, *405*, 764−767.
(58) Roch, N.; Florens, S.; Costi, T. A.; Wernsdorfer, W.; Balestro, F. Observation of the Underscreened Kondo Effect in a Molecular Transistor. *Phys. Rev. Lett.* **2009**, *103*, 197202.
(59) Parks, J. J.; Champagne, A. R.; Costi, T. A.; Shum, W. W.; Pasupathy, A. N.; Neuscamman, E.; Flores-Torres, S.; Cornaglia, P. S.; Aligia, A. A.; Balseiro, C. A.; Chan, G. K.-L.; Abruña, H. D.; Ralph, D. C. Mechanical Control of Spin States in Spin-1 Molecules and the Underscreened Kondo Effect. *Science* **2010**, *328*, 1370−1373.
(60) Schleyer, P. v. R.; Maerker, C.; Dransfeld, A.; Jiao, H.; van Eikema Hommes, N. J. R. Nucleus-Independent Chemical Shifts: A Simple and Efficient Aromaticity Probe. *J. Am. Chem. Soc.* **1996**, *118*, 6317−6318.
(61) Geuenich, D.; Hess, K.; Köhler, F.; Herges, R. Anisotropy of the Induced Current Density (ACID), a General Method To Quantify and Visualize Electronic Delocalization. *Chem. Rev.* **2005**, *105*, 3758−3772.

https://doi.org/10.1021/jacs.2c02700
J. Am. Chem. Soc. 2022, 144, 12725−12731